ISSN : 0974 - 7540 Volume 4 Issue 2

Trade Science Inc.

Research & Reviews On Electrochemistry

Full Paper

RREC, 4(2), 2013 [61-71]

Electrochemical sensing of some dicarboxylic aliphatic acids on glassy carbon electrode modified with electrodeposited platinum nanoparticles

Farouk A.Rashwan, Mahmoud El-Rouby*

Chemistry Department, Faculty of Science, Sohag University, Sohag, 82425, (EGYPT)

E-mail: dr_mahmoudelrouby@hotmail.com

ABSTRACT

Electroreduction of oxalic, succinic, tartaric and malic acid in aqueous KCl on glassy carbon electrode (GCE) immobilized with nanoparticles of platinum was investigated. Platinium nanoparticle (Pt_{NPs}) - modified electrodes were prepared by the electrodeposition with cyclic voltammetric method onto glassy carbon electrode. The surface morphology of the electrodeposited Pt nanoparticles was examined by SEM. Also, the electrochemical properties of the prepared electrodes were investigated with different electrochemical techniques; cyclic voltammetry, chronoamperometry, and electrochemical impedance spectroscopy. The Pt-nanostructured film on GCE exhibits an ability to improve dramatically the current intensity of the cyclic voltammograms of the reduction behavior of all acids under investigation. Instead of irreversible ill-defined waves obtained on bare GCE, combined with Pt-nanoparticles, the monolayer-modified electrode (Pt/GCE) gives sensitive reversible responses. Obviously, this improvement returns to the electrocatalysis of the electron transfer between the acids and the new modified electrode. Electrochemical impedance spectroscopy at a fixed potential was performed at treated GCE. The mechanism of the electrode reactions and the equivalent circuits of the GCE for the different acids have been proposed. The different CV and EIS parameters in addition to the charge transfer rate constants associated with the redox processes of the acids are evaluated and discussed.

KEYWORDS

Electrodeposition;
Pt nanoparticles;
Electroreduction;
Dicarboxylic acids.

INTRODUCTION

Nanosized particles attracted much attention, and are currently the subjects of considerable research programs. Due to their high specific surface area which makes it having unusual physical and chemical properties, nano-materials are used in the potential application and chemical separation[1]. Also, nanoparticles have been found to be used in technological applications in many different areas, such as photocatalysis[2], electrocatalysis[3], and biomedical applications[4,5]. The electrodeposition of metal nanoparticles onto carbon electrodes has become the interest of a large number of researches, due to their catalytic activity toward reac-

tions of interest[6-10]. This can be attributed to that, carbon electrodes are characterized by the high chemical inertness as well as low oxidation rate in addition to small gas and liquid permeability[11]. Electrochemical deposition conditions of metal are easy to alter, enabling creation of a wide range of electrodes with nanoparticles of differing sizes, shapes, and distributions. The procedure is rapid, simple, and reproducible, more than viable alternative to the time-consuming and delicate production of an electrode via colloidal platinum[12].

Electrodeposition of platinum deposits produced during the electroreduction of $PtCl_6^{2-}$ complex in aqueous solutions has a much enhanced surface[13-15]. Catalytic activity is one of the most important properties of Pt nanoparticles; therefore, it is used to enhance the reaction efficiency. Due to the biological and industrial importance of the biological acids under investigation, the electrochemical behavior of them was studied in this article. Furthermore, little studies covering the area of those acids concerning their electroreduction have been carried out[16,17]. Moreover, almost totally rare studies using GCE immobilized with Pt nanoparticles were undertaken. Recently, the reduction of carboxylic acids has been categorized according to reaction mechanism and their pK_a in dimethyl sulfoxide at platinum electrodes[17]. In the present work, an application of the relatively new trend of modifying electrodes is displayed. Accordingly, detailed investigations of the electroreduction behavior of oxalic, succinic, malic and tartaric acids in a 0.1 mol L^{-1} KCl on Pt-nanoparticle electrodeposits are carried out. Cyclic voltammetric, electrochemical impedance, and related techniques were combined to obtain the desired data.

EXPERIMENTAL SECTION

Oxalic. malic, tartaric, succinic acids, potassium hexacyanoferrate (III), KCl and Na_2SO_4 were purchased from BDH and di-hydrogen tetrachloroplatinate from Aldrich. Stock solutions 0.1 mol L^{-1}, were freshly prepared by dissolving the appropriate amounts in bidistilled water.

All electrochemical measurements were performed with an EG&G PARC Potentiostat/Galvanostat model 273 A. The EIS measurements were performed with a lock-in analyzer (Model 5208) coupled with the potentiostat/galvanostat (model 273 A). The models 378 and software are used for EIS and CV measurements respectively. A conventional three-electrode cell system was used, consisting of a bare or modified glassy carbon (3 mm in diameter) as a working electrode, platinum sheet as an auxiliary electrode, and the Ag/AgCl as the reference electrode. All experiments were thermostated at 298 ± 0.2 K using a Huke model. Surface analysis of the modified electrodes were carried out using a JEOL JSM-5500 LV Scanning Electron Microscope (JOEL, Japan), at an acceleration voltage of 5 keV and a working distance of 4–5 mm. Image analysis were performed visually and with common software (ImageJ, Wright Cell Imaging Facility, Toronto Western Research Institute, University Health Network) for particle counting and particle size.

Preparation of the modified electrode with Pt nanoparticles

Prior to the electrodeposition of Pt nanoparticles, the glassy carbon electrode surface was polished first with no. 2000 emery paper, then with aqueous slurries of successively finer alumina powder with the help of polishing microcloth. Then, it was rinsed with doubly distilled water. The bare GCE was then, sonicated for 10 min in bidistilled water bath. Electrodeposition process was accomplished as in our previous published article[15]. A reversible cyclic voltammogram for the reduction of Pt (IV) on the GCE is observed at -0.42 V versus Ag/AgCl. This wave is attributed to the reduction of Pt (IV) to the Pt metal on the surface of the GCE[5,15,18]. After platinum deposition, the electrode was cleaned by double distilled water. And the stability of the electrode towards the electroreduction of the acids was measured by comparasion the peak current height and the behavior of the cylic voltammogaram of reference material of known behavior such as ferri/ferrocyanide.

RESULTS AND DISCUSSION

Pt nanoparticles characterization

Scanning electron microscopy analysis characterization

Scanning electron microscopy (SEM) images of the Pt nanoparticles electrodeposited onto the GCE under

different operating conditions are shown in Figure 1a-d. The SEM images show that the deposited Pt particles are in the nanoscale size and homogeneously distributed throughout the surface of GC Electrode.

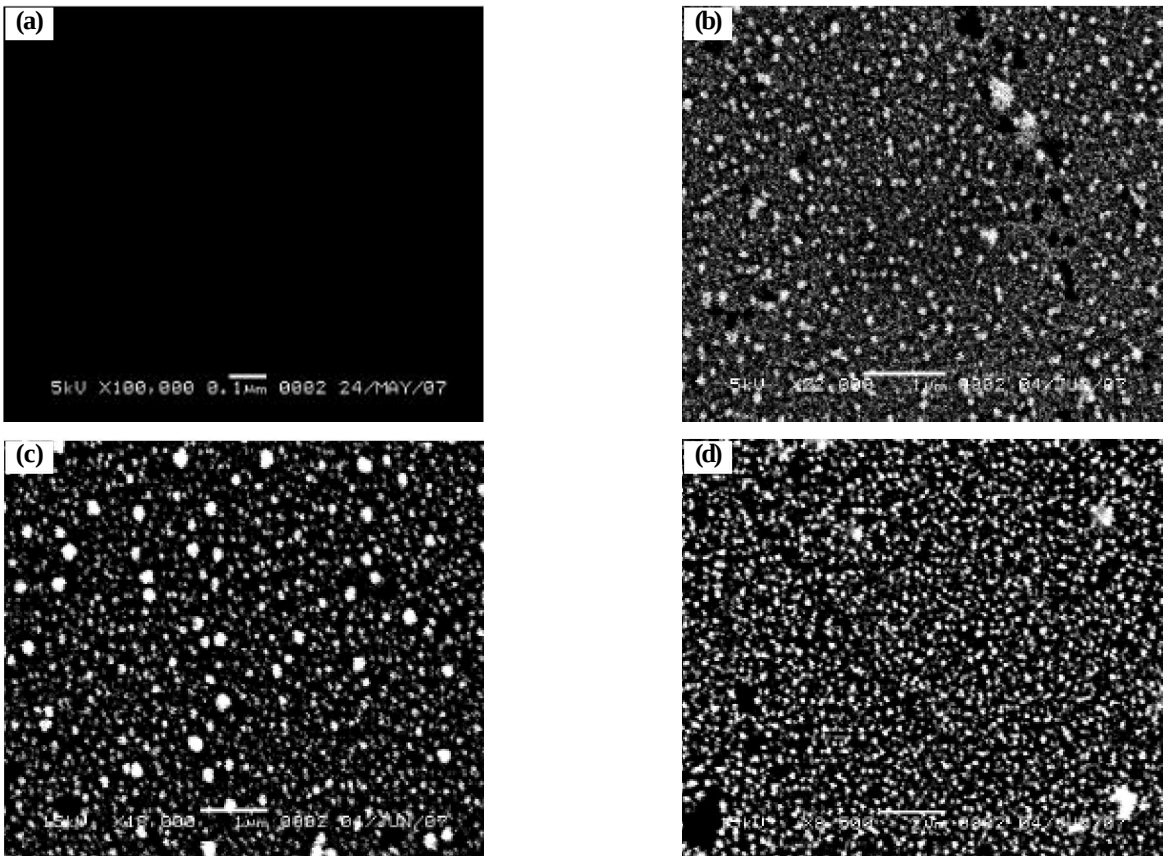

Figure 1 : SEM images of bare GCE (a) and electrochemically deposited Pt Nanocrystallites on GCE; delay time 0 s and 0.5 mmol L^{-1} H_2PtCl_6 solution, (b); Delay time 60 s and 0.5 mmol L^{-1} H_2PtCl_6 solution, (c) Delay time 0 s and 1 mmol L^{-1} H_2PtCl_6 solution.(d) at 298 k.

The Pt nanocrystals in the SEM images appear as circular bright spots surrounded by a textured background of darker GC substrate. It is clear from these images that the increase of either the delay time of deposition or the concentration of the $PtCl_6^{2-}$ resulted in an increase in the average particle size of the Pt nanoparticles, and as confirmed by the precise calculations of the ImageJ program. It has been shown that the low concentration bath (0.5 mmol L^{-1} H_2PtCl_6), yields a low number density with a lot of nanocrystals (~ 70%) with small size (~ 10 nm). The other particles having 20 nm average sizes (Figure 1b). At the higher concentration (1.0 mmol L^{-1} H_2PtCl_6), a high number density of relatively monodisperse particles are deposited with increasing the size. Small size particles (~ 32 nm) of ~ 49% coexisting with small number (~10%) of large size particles (~ 68 nm) and 20% of a size (~120 nm), as shown in Figure 1d. This reflects both an increase of the active sites on the surface of GCE (increasing the Pt loading) and nucleation growth.

The increase of the deposition time from 0 to 60 s leads to both an increasing in the particle size and an increasing in the particle number density. A 30% of large size particles have 60–88 nm range, and a 17% of the particles have 150–300 nm size range, these large particles are observed coexisting with lots of (~ 53%) smaller size nanoparticles (~15 nm) as shown in Figure 1c. This means that the nucleation growth is favored over the establishment of new deposition active sites. SEM image analyses for nanoparticles are summarized in TABLE 1. Furthermore, both the real surface area of the Pt loading on GCE/cm^{-2} and the mass specific surface area (cm^2 μg^{-1}), were calculated by two methods, such as SEM analysis and mass transfer method. The data of both methods are found to be in agreement with each other.

Full Paper

TABLE 1 : Physical characteristic parameters determined from voltammetric measurements and SEM analysis for Pt nanoparticles electrodes.

Electrode no.	(1*) Q (μC)	(2*) Pt loading (g cm^{-2}) × 10^5	(3*) Real surface area of Pt loading (cm^2)		(4*) Specific surface area (cm^{2}μg^{-1})		(5*) Roughness factor	(7*) Mean Diameter, nm
			SEM method	Mass transfer method	SEM method	Mass transfer method		
B	636.68	1.79	1.20	1.30	94.82	95.61	3.13	15 ± 2
C	772.91	2.21	1.46	1.44	93.25	89.00	2.50	38 ± 2
D	878.43	2.51	1.60	1. 80	90.20	71.57	1.88	180 ± 2

(1*) Net cathodic charge passed in metal deposition; (2*) calculating the metal loading assuming 100% current efficiency; (3*) As estimated from SEM analysis and mass transfer methods; (4*) Mass specific surface area: Surface area per unit weight of the loaded metal; (5*) Surface area of the metal deposits per unit area of the GCE; (6*) and (7*) data measurements based on Imagej program software.

Cyclic voltammetric characterization of the modified GCE with Pt_{NPs}

Cyclic voltammetric measurement with the standard electroactive species $Fe(CN)_6^{3"/4"}$ are used to test the validity of the prepared electrodes and the kinetic barrier of the interface. This method is frequently used to estimate the real active surface area of the electrodes. Figure 2 shows CV response on the bare and the modified GC with Pt nanoparticle in aqueous 0.1 mol L^{-1} KCl solution containing 5 mmol L^{-1} $[Fe(CN)6]^{4"/3"}$ with scan rate equal to 50 mV s^{-1} at 298 K. The well-defined cyclic voltammograms, at the modified GCE with a peak-to-peak separation (ΔE_p) of about ~ 0.070 V vs. Ag/AgCl are observed (Figure 2b- c- d). An obvious increase in the anodic and the cathodic peak currents are also observed as both the Pt loading and the particle size of the deposits decreased. This is due to high surface area enhancing the electron transfer. A peak-to-peak separation (ΔE_p) of 0.318 V vs. Ag/AgCl is obtained when the bare GCE is used, (Figure 2a). A decrease in both the anodic and cathodic peak currents compared with those observed in case of the modified electrodes is also observed. Hence, the electron transfer becomes faster after modification of the GCE with the Pt nano particles.

Characteristic parameters for the electrochemical measurement of $K_3[Fe(CN)_6]$ at the different loads of GCE/Pt_{NPs} are also calculated and summarized in TABLE 1. The specific surface areas (cm^2 μg^{-1}) of the fabricated electrodes were calculated by using the relation[19];

$$S = \frac{100\ A_{rsa}}{W\ A_{gsa}} \qquad (1)$$

Where; S is the specific surface area of the electrode, A_{rsa} is the real surface area in cm^2, W is the amount of the loaded metal (μg cm^{-2}) and A_{gsa} is the geometric surface area of the glassy carbon electrode.

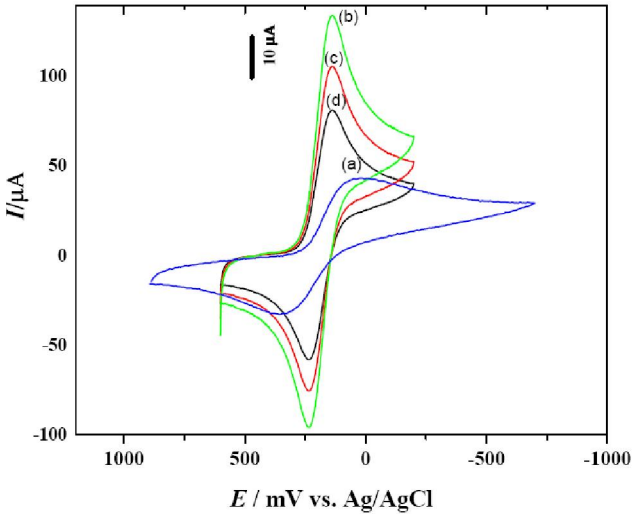

Figure 2 : CV of 5 mmol L^{-1} $[Fe(CN)_6]^{-3/-4}$ in 0.1 mol L^{-1} KCl, at v = 50 mV s^{-1} at 298 k, on bare (a) modified GCE with Pt_{NPs} at different loads of; 1.79×10^{-5} (b), 2.21×10^{-5} (c) and 2.51×10^{-5} g cm^{-2} (d).

The real surface area of the loading metal on the GCE was estimated by SEM analysis and by Mass transfer method. The Mass transfer method is estimated by using the relation of Randles[20-22];

$$I_p = -3.01 \times 10^5\ n^{3/2}\ \alpha^{ap1/2}\ D^{1/2}\ A_{rsa}\ c_o\ |v|^{1/2} \qquad (2)$$

Where I_p is the peak current in Amperes (A), n the number of the electrons participating in the redox reaction, α the apparent electron transfer coefficient, D the diffusion coefficient in cm^2 s^{-1}, A_{rsa} the real surface area of the modified electrode in cm^2, c_o the bulk concentration of the species in mole cm^{-3} and v is the potential sweep rate in V s^{-1}.

The plot of I_p versus $v^{1/2}$ yields the real surface area of the loaded metal on the GCE. A linear increase in the peak height with increasing the square root of the scan rate is observed. Thus, the electron transfer process is controlled via diffusion phenomena. This implies that these nanoparticles provided the necessary conduction pathways in promoting the electron transfer between the analyte and the electrode surface.

The value of the electron transfer coefficient is assumed to be α H" 0.5 for ferri/ferrocyanide redox couple and by subsequent determination of diffusion coefficient (D) from amperometric measurements, the heterogeneous charge transfer rate constant (k_s) can be obtained according to equation (3)[19];

$$\psi = \frac{(D_0/D_R)^{\alpha/2} k}{\pi D_0 \nu (nF/RT)^{1/2}} \quad (3)$$

The mean value of k_s on the modified Pt_{NPs} electrodes is found to be equal to 0.11 cm s^{-1} indicating that the reaction is occurring fastly on the modified electrodes compared with that occurring on the bare electrode.

Chronoamperometric characterization

Figure 3 shows the chronoamperograms of 5 mmol L^{-1} $K_3[Fe(CN)_6]$ in 0.1 mol L^{-1} KCl on the GCE/Pt_{nano} with different Pt loadings. The first and the second working electrode potentials are adjusted at 0.600 and 0.128 V (vs Ag/AgCl), respectively. The diffusion coefficient can be obtained by using the relation between current decay and time as in Cottrell equation (4);

$$I = n FA D^{1/2} c_o \pi^{-1/2} t^{-1/2} \quad (4)$$

Where n is the number of electrons transferred, F the faraday constant (96484 C mol^{-1}), A the electrode surface area (cm^2), c_o the bulk concentration of species (mol cm^{-3}), i the current (A), t the time elapsed (s) and D the diffusion coefficient (cm^2 s^{-1}).

The plots of $It^{1/2}$ vs. t for a specific concentration of ferricyanide show that, $It^{1/2}$ function is constant and time independent over a wide range of time, indicating that the electron transfer process is diffusionally controlled. In addition, the catalytic rate constant (k_{cat}) for ferricyanide on the GCE/Pt_{nano} has been calculated using Galus method; by using the equation (5)[19];

$$\frac{i_{cat}}{i_l} = \pi^{1/2} (k_{cat} C_o t)^{1/2} \quad (5)$$

Where i_{cat} is the catalytic current of ferricyanide on the modified electrode, i_l the limiting current in absence of ferricyanide, c_o the concentration (mol cm^{-3}) and t the time in second. The slope of I_{cat}/I_l vs. $t^{1/2}$ gives k_{cat} mean value of a 3.98×10^3 M^{-1} s^{-1}. This points out to the high catalytic activity of the modified electrode towards the electroreduction of ferricyanide ions.

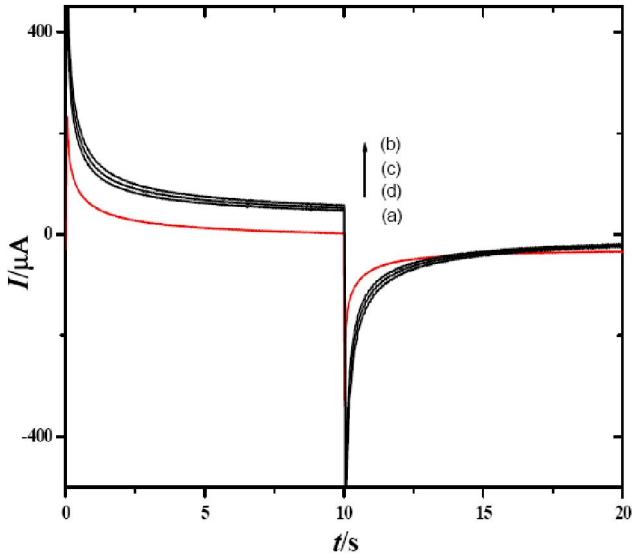

Figure 3 : Double step potential chronoamperograms of 5 mmol L^{-1} $K_3[Fe(CN)_6]$ in 0.1 mol L^{-1} KCl obtained on bare (a) and modified GCE with Pt_{NPs} at τ = 10 s at 298 K, with different loads of Pt_{NPs}; 1.79×10^{-5} (b), 2.21×10^{-5} (c) and 2.51×10^{-5} g cm^{-2} (d).

Electrochemical impedance spectroscopic (EIS) characterization

EIS is an effective and very sensitive method for probing the features of the surface of modified electrodes, and to further investigate the impedance changes of the electrode surface on the modified electrodes. To investigate the electrical properties of the electrodes / solution interfaces, the Randle's equivalent circuit can be chosen to represent the system under investigation.

As shown in Figure 4, the EIS spectra presented as Nyquist plot for the bare GCE and for the modified electrode having different loading of Pt Nanoparticles for 5 mmol L^{-1} ferricyanide in 0.1 mol L^{-1} KCl at the cathodic peak potential at 298 K. It is clear from the Figure that, charge transfer resistance (R_{ct}) has the greatest value ~ 2100 Ω for the bare GCE in the test solution. The R_{ct} decreased dramatically to ~ 200 Ω as the electode being modified with Pt nanoparticles. It can be concluded from the Figure that, when the Pt loading is increased (large particle size), the R_{ct} increased.

Moreover, at modified electrodes, the data demonstrate that at low measured frequencies a linear impedance locus with an angle of ~45° to the real axis. At high measured frequencies, there a partially small resolved semicircle is observed. This implies that the Pt nanoparticles play an important role in the kinetics of charge transfer process. At electrode (b), linear impedance (Warburg impedance, Z_w) with an angle of ~45° to the real axis at all measured frequencies is observed. This can be attributed to the relaxation occurring at the electrode/solution interface and supports the diffusion controlled charge transfer process. These data showed that the Pt nanoparticles have been successfully attached to the GCE electrode surface, and the electrode gets working with high efficiency. This is also in agreement with the results of cyclic voltammetric measurements.

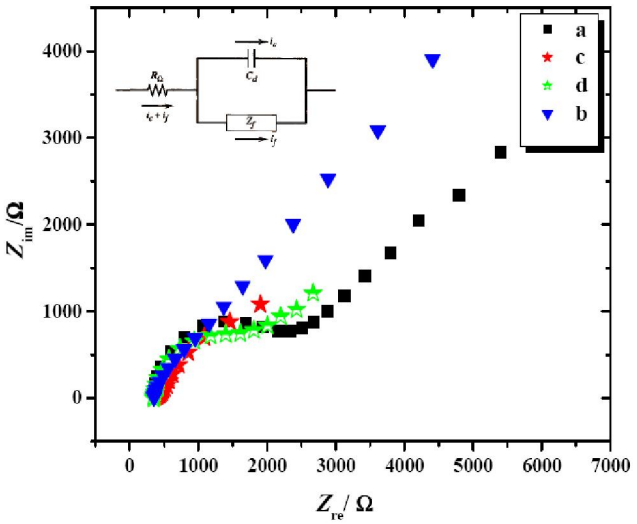

Figure 4 : Complex impendence plane plots for 5.0 mmol L^{-1} $Fe(CN)_6^{3"/4"}$ in 1.0 mol L^{-1} KCl, on bare (a), and modified GCE with Pt_{NPs} with different loads of; 2.21×10^{-5} g cm^{-2} (b) 2.51×10^{-5} g cm^{-2} (c) and 1.79×10^{-5} g cm^{-2} (d).

Electrochemical response of di-carboxylic acids on the Pt nanoparticles

Cyclic voltammetry (CV)

The CV investigations indicate that the nanoparticles have cleary improved the electroreduction behavior of these acids and led to large increase in the current and enhanced behavior is obtained compared to the bare GCE. The voltammograms for all acids is stable during 20 cycles scanning. Cyclic voltammograms of 1.25 mmol L^{-1} oxalic, succinic, malic and tartaric acids in a 0.1 mol L^{-1} KCl at 298 K with scan rate of 100 mV s^{-1} are shown in Figure 5 and Figure 6. The first voltammograms which is not defined and appeared absolutely not separated from that of the decomposition of the solvent is taken on the bare GCE (Figure 5). The other plots in Figure 6 are the CV responses taken on modified GCE with Pt nanoparticles. The small broad pre-cathodic peaks are appeared on the modified GCE with nanoparticles in the case of succinic, malic and tartaric acids. These small pre-cathodic peaks are concluded to be due to the reduction of the dissociated protons of these acids that can be adsorbed on the surface of the electrode and then exploited in the following discharge process. Since in the acidic medium, the reaction begins easly with the reduction of the dissociated protons. These voltammograms exhibit reversible and enhanced behavior for all acids compared with the behavior at the bare GCE. The reversibility of the electroreduction process on the Pt-nanoparticles / GCE is tested through the peak current ratio (i_{pa}/i_{pc}) peak potential separation ("$E_p = E_{pc} - E_{pa}$ or $E_p - E_{p/2}$) and the current function ($i_p/v^{1/2}$) diagnostic criteria. All the parameters of the electroreduction of the acids under investigation on GCE modified with Pt nanoparticles are summarized in TABLES 2-5.

These data confirm that the process occurring on the GCE modified with Pt-nanoparticles is nearly reversible one electron transfer process at the main cathodic peak according to the calculations of Nicholson and Shain[23].

$$\left|E_p - E_{p/2}\right| = \frac{2.2\,R\,T}{n\,F} = \frac{56.5}{n}\ \text{mV} \qquad (6)$$

Both of the linear responses obtained for i_p-$v^{1/2}$ relation (Figure 7) and for the relation resulting from the increase in the peak height with the increase in concentration of the acids (Figure 8) at milimolar levels (i.e. 1, 2, 3, …. to 8 mmol L^{-1}) reveal that the electron transfer process on the modified electrode is controlled via diffusion phenomena. Furthermore the criterion of the current function ($i_p/v^{1/2}$) which decreases slightly with increasing the scan rate as shown in TABLES 2-5, ensures the presence of a chemical reaction following the electron transfer process (EC mechanism) in that case[23]. The electroredction of the acids differ in the location of their cathodic peaks. The cathodic peak of succinic acid is shifted to more negative direction more than that of oxalic, malic and tartaric acids. This difference can be

explained on the basis of the presence of the methelene - $(CH_2)_2$- donating groups, that delays the process of electroreduction of succinic acid, the same reason in malic and tartaric acids.

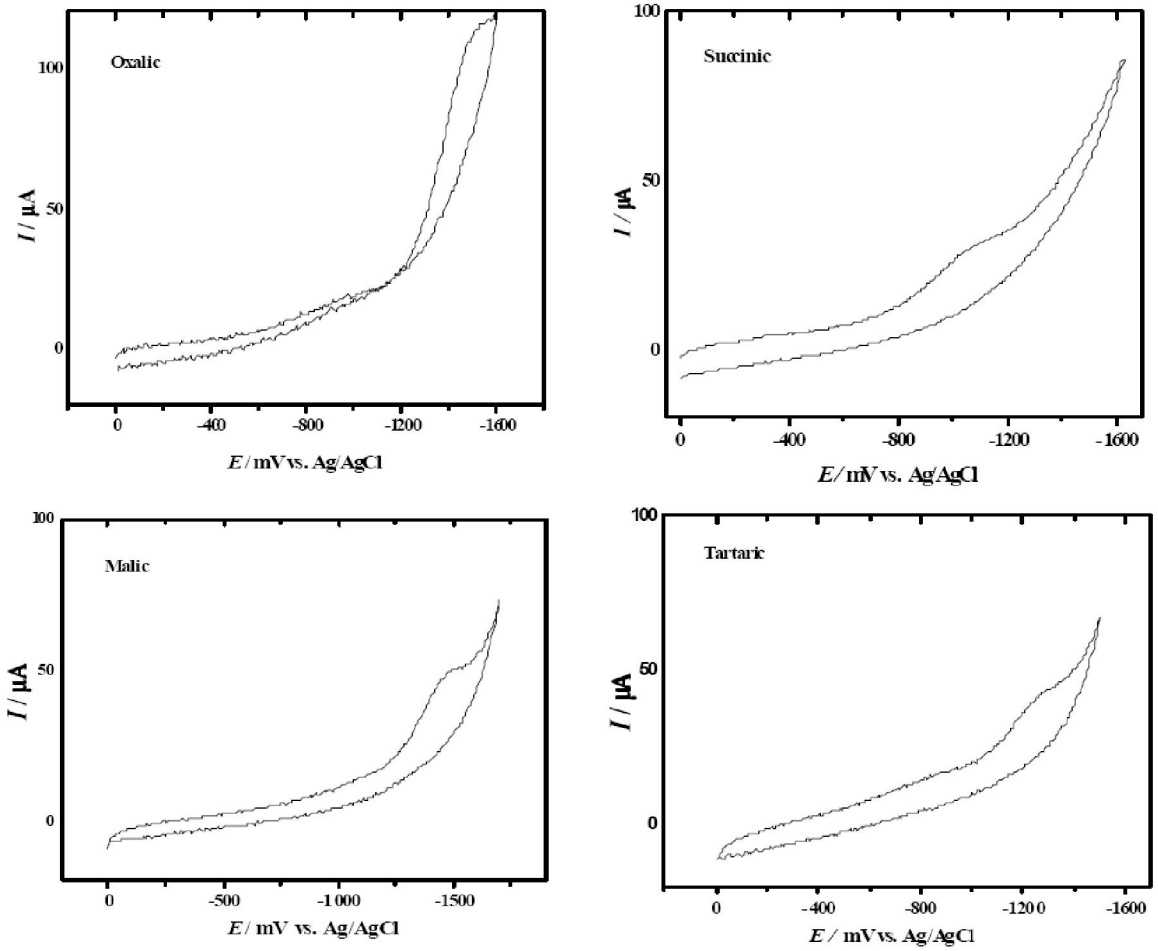

Figure 5 : CVs of 1.25 mmol L^{-1} oxalic, succinic, malic and tartaric acid in 0.1 mol L^{-1} KCl at 298 K, at v = 100 mV s^{-1}, on bare GCE.

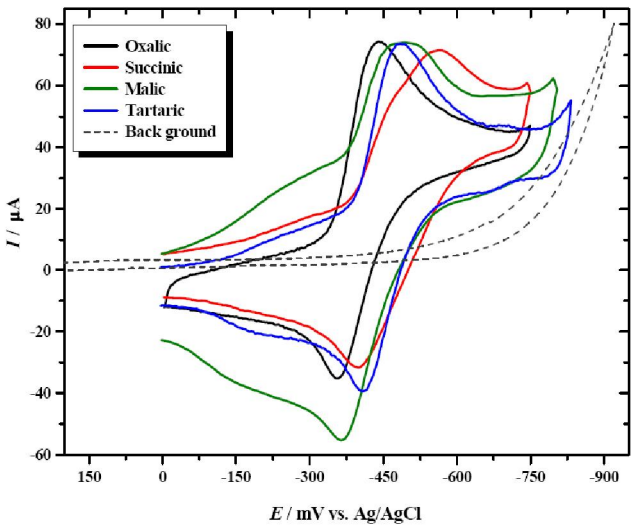

Figure 6 : CVs of 1.25 mmol L^{-1} oxalic, succinic, malic and tartaric acid in 0.1 mol L^{-1} KCl at 298 K, at v = 100 mV s^{-1}, on modified GCE with Pt_{NPs} at loads of 1.79×10^{-5} g cm^{-2}.

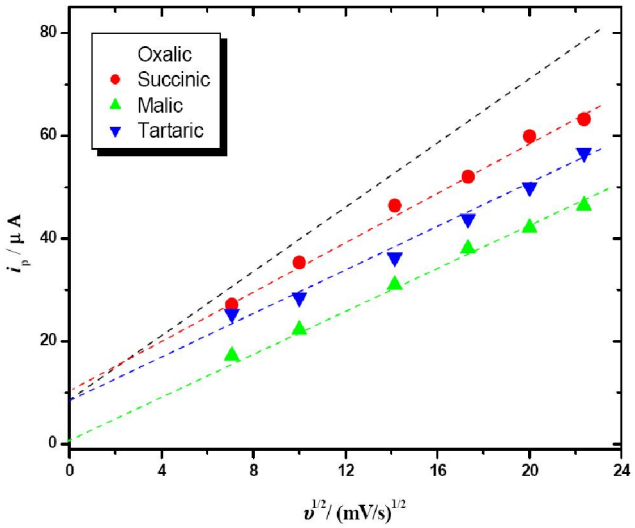

Figure 7 : Correlation between i_{pc} vs. $v^{1/2}$ for the electroreduction of 1.25 mmol L^{-1} oxalic, succinic, malic and tartaric in a 0.1 mol L^{-1} KCl at modified GCE with Pt_{NPs}.

Full Paper

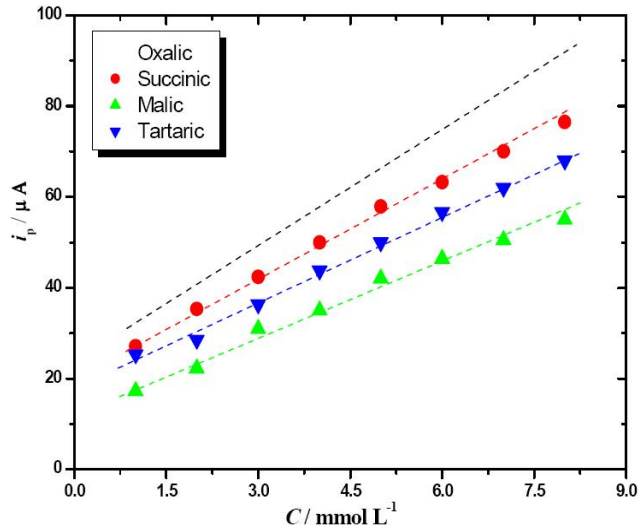

Figure 8 : Correlation between i_{pc} vs. concentrations for the electroreduction of oxalic, succinic, malic and tartaric acids in a 0.1 mol L^{-1} KCl at modified GCE with Pt_{NPs}.

TABLE 2 : CV data for the electroreduction of 1.25 mmol L^{-1} oxalic acid a in 0.1 mol L^{-1} KCl on the GCE/ Pt_{NPs} at 298 K.

Scan rate (Vs^{-1})	$-E_p^c$ (V)	i_p^c (μA)	i_p^a/i_p^c	ΔE_P (mV)	$i_p/v^{1/2}$ (μAmV^{-1}s$^{1/2}$)
0.05	0.438	41.50	0.78	83.30	5.87
0.10	0.441	57.39	0.99	97.30	5.74
0.20	0.454	70.74	1.32	115.30	5.00
0.30	0.464	84.00	1.35	125.30	4.84
0.40	0.469	94.10	1.39	130.80	4.70
0.50	0.476	103.80	1.40	146.80	4.64

TABLE 3 : CV data for the electroreduction of 1.25 mmol L^{-1} succinic acid on the GCE/ Pt_{NPs} in a 0.1 mol L^{-1} KCl at 298 K.

Scan rate (Vs^{-1})	$-E_{pc}$ (V)	i_{pc} (μA)	i_{pa}/i_{pc}	ΔE_P (mV)	$i_p/v^{1/2}$ (μAmV^{-1}s$^{1/2}$)
0.05	0.493	27.10	0.99	157.00	3.833
0.10	0.500	35.30	1.05	179.66	3.530
0.20	0.507	46.40	1.03	195.95	3.281
0.30	0.523	52.00	1.10	206.00	3.002
0.40	0.529	59.88	1.10	216.20	2.994
0.50	0.534	63.20	1.15	222.52	2.826

TABLE 4 : CV data for the electroreduction of 1.25 mmol L^{-1} malic acid on the GCE/ Pt_{NPs} in a 0.1 mol L^{-1} KCl at 298 K.

Scan rate (Vs^{-1})	$-E_p^c$ (V)	i_{pc} (μA)	i_{pa}/i_{pc}	ΔE_P (mV)	$i_p/v^{1/2}$ (μAmV^{-1}s$^{1/2}$)
0.05	0.476	17.21	1.96	108.87	2.430
0.10	0.494	22.22	1.69	133.10	2.220
0.20	0.516	30.96	2.03	177.40	2.198
0.30	0.522	38.00	1.99	198.34	2.190
0.40	0.539	42.07	2.14	210.07	2.100
0.50	0.559	46.40	2.06	220.37	2.075

TABLE 5 : CV data for the electroreduction of 1.25 mmol L^{-1} tartaric acid on the GCE/ Pt_{NPs} in a 0.1 mol L^{-1} KCl at 298 K.

Scan rate (Vs^{-1})	$-E_{pc}$ (V)	i_{pc} (μA)	i_{pa}/i_{pc}	ΔE_P (mV)	$i_p/v^{1/2}$ (μAmV^{-1}s$^{1/2}$)
0.05	0.473	25.35	0.93	73.90	3.585
0.10	0.483	28.55	0.85	80.90	2.855
0.20	0.496	36.35	0.91	90.60	2.570
0.30	0.504	43.80	0.94	108.22	2.528
0.40	0.510	50.00	0.92	115.50	2.500
0.50	0.515	56.65	0.94	120.32	2.469

Heterogeneous charge transfer rate constant (k) for the electroreduction, can be easily obtained with the aid of the equation (3)[19]. The value of the electron transfer coefficient is assumed to be H" 0.5 for this system. The value of k_s for the electroreduction of oxalic, succinic, malic and tartaric acids under these conditions amounts to 0.59, 0.20, 0.225 and 0.27 cm s^{-1} on Pt_{NPs} electrode respectively. This is supporting the fact that the reaction on the GCE/Pt_{NPS} is facile on the surface of the modified electrode for these acids under those modified conditions uder the following sequence; oxalic > tartaric > malic > succinic. It can be concluded that, the possible route for the electroreduction mechanism of the acids on the glassy carbon electrode modified with platinum nanoparticles is that the acid receives one electron from the electrode to form the radical anion. This radical anion is passing though a chemical reaction, dimerization, (EC mechanism). The dimerization of dicarboxylic acids can be achieved by applying a negative potential in acidic medium via attachment of the carboxylic group[24]. The resultant dimer radical anion can be protonated with one proton. The expected route for the electroreduction mechanism is assumed as follow;

$$A + e \rightleftharpoons A^{\cdot -} \xrightarrow{A} [A\text{-}A]^{\cdot -} \qquad (7)$$

Where A and $A^{\cdot -}$ is the neutral oxalic and its radical anion, respectively and $[A\text{-}A]^{\cdot -}$ is the dimer radical anion of the acid.

Electrochemical impedance spectroscopic measurements (EIS)

Figure 9 shows the Nyquist plots of the impedance spectroscopic diagram on the Pt nanoparticle electrode of oxalic, succinic, malic and tartaric acids are measured at frequencies of 5 Hz to 100 kHz at the cathodic peak potential of the acids under investigation. The way of Nyquist plots at low frequencies resemble Warburg

impedance due to diffusional control of AC response for all acids. The Randles equivalent circuit is not sufficient for the description of the process in this case, thus it should be assumed the presence of an additional impedance contribution due to the coupled chemical reaction following the electron transfer process. The Ohmic resistance of the solution (R_s), the charge transfer resistance (R_{ct}) at the electrode surface and the double layer capacitance (C_{dl}), were calculated using the Bode plots (Figure 10) that listed in TABLE 6. The R_{ct} in the case of oxalic acid is considerably small; this is due to the catalyzing effect of the Pt_{Nps} and there are no effecting groups as in the rest of the acids. The relatively high C_{dl} value is consistent with the foregoing concept. Also the charge transfer process in case of the acids is somewhat slower than that of the corresponding oxalic acid. The R_{ct} in the case of tartaric acid is found to be higher than the corresponding of oxalic acid at the modified electrode, whereas the C_{dl} is clearly less than that of oxalic acid but more than that of malic and succinic acids confirming the forgoing results.

The EIS is also used for the calculation of the heterogeneous rate of electron transfer, by the aid of the reduced equation[25-27];

$$\cot \phi = 1 + \frac{\sqrt{D}}{2k_s}\sqrt{\omega} \qquad (8)$$

where ϕ is shift of the phase angle, D the diffusion coefficient of species, assuming that both redox forms have the same D, k_s the heterogeneous rate constant of the electron transfer and ω the angular frequency of the sinusoidal current and assuming $\alpha = \beta = 0.5$. The dependence of the cotangent of ϕ with $\omega^{1/2}$; indicates that deviation from the linearity at low frequencies can be detected, indicating the presence of a chemical reaction following the charge transfer process (EC).

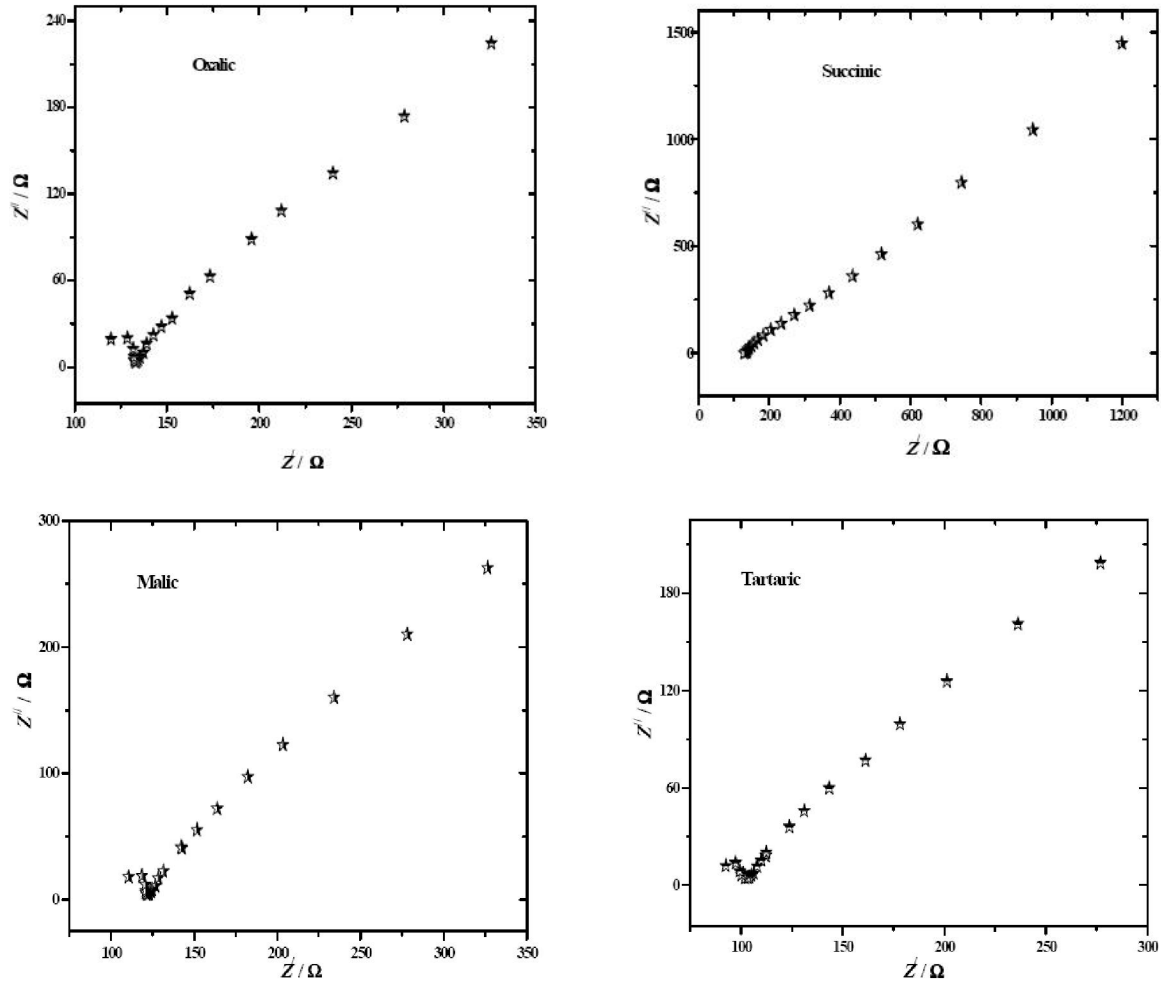

Figure 9 : Complex impendence plane plots, for 1.25 mmol L^{-1} oxalic, succinic, malic, tartaric acid in a 0.1 mol L^{-1} KCl, AC amplitude at 0.005 V, frequencies from 100 KHz to 5 Hz at 298 K, on GCE modified with Pt_{NPs}.

Full Paper

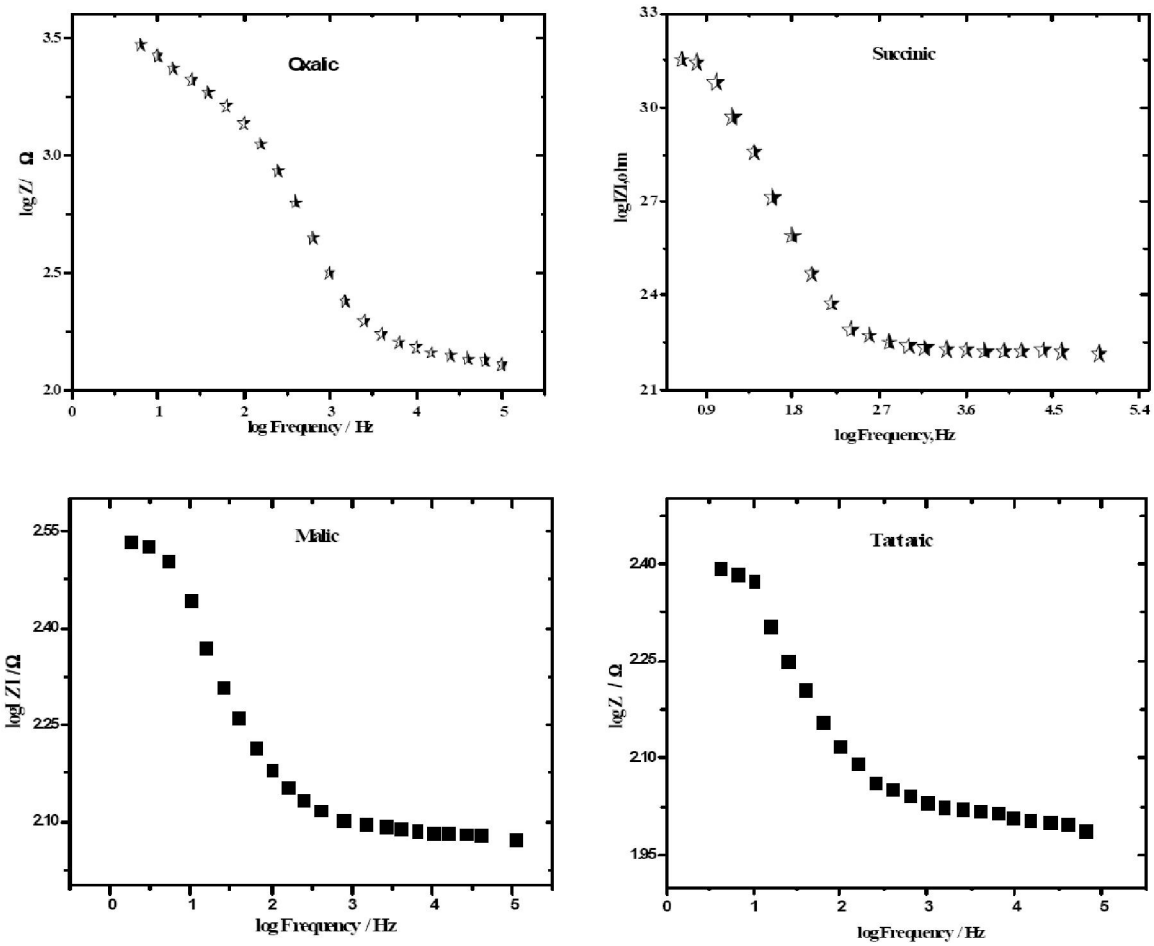

Figure 10 : Bode plots obtained for Pt_{NPs} in a 0.1 mol L^{-1} KCl and 1.25 mmol L^{-1} of oxalic, succinic, malic and tartaric acid at E_p vs. Ag/AgCl.

TABLE 6 : EIS data was obtained for the electroreduction of 1.25 mmol L^{-1} oxalic, succinic, malic and tartaric acids at GCE modified with Pt nanoparticles.

Acid	R_s, Ω	R_{ct}, Ω	$C_{dl.}$ f × 10^{-5}	angel, ϕ
Tartaric	131.00	80.10	150.00	42.70
Malic	124.67	46.50	132.00	45.74
Succinic	147.88	200.64	50.60	44.16
Oxalic	132.45	50.10	248.00	46.93

The heterogeneous rate constant values of the electron transfer reaction for the electroreduction of oxalic, succinic, malic and tartaric acids are obtained by this method, having the value 0.57, 0.25, 0.24 and 0.29 cm s^{-1} respectivily. These values are consistent with that obtained from CV measurements, and it falls within the range of the diffusion controlled process values confirmed by CV measurements.

Dependence of the peak potential (E_p) on the pK_{a1} of the acids

Since the electroreduction mechanism of the carboxylic acids on the modified electrode under investigation involves the uptake of protons in most cases, the E_p is correlated with pK_{a1} values in aqueous media. So, this relation can be used to estimate the pK_{a1} of new acid derivatives from the corresponding E_p. It turns out to be possible to use the main reduction process to simplify the situation for the practical application proposed in this study.

Figure 11 shows the plots of E_p against the first dissociation constant of the acids (pK_{a1}) obtained in aqueous media[28]. As long as the acids have the same functional group, there is a linear relationship between cathodic E_p and the pK_{a1} obtained in aqueous media. But the acids having different groups exhibit different slopes. When the cathodic E_p data are plotted against pK_{a1} in corresponding media, good straight line with correlation coefficient (R) of 0.996 is obtained irrespective of the functional groups of the acids. The slope is about 0.046 V per pK_{a1} unit and with different intercepts as by the data inserted in the Figure.

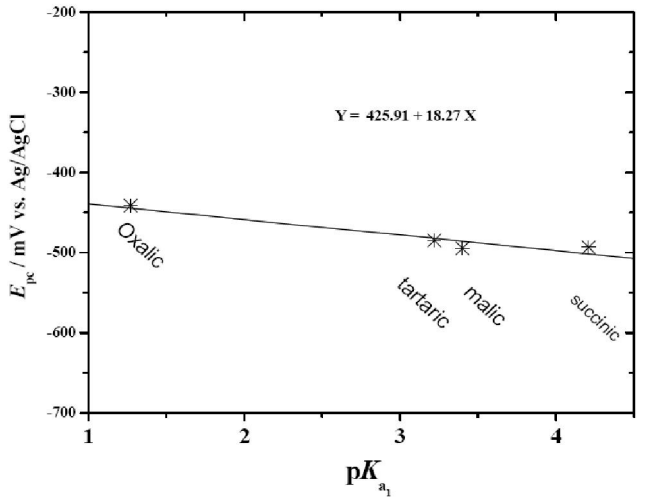

Figure 11 : Linear correlation between pK_{a1} of 1.25 mmol L^{-1} of the acids in 0.1 mol L^{-1} KCl for the selected acids and their cathodic peak potential values at v = 100 mV s^{-1} at 298 K on the modified GCE with Pt_{NPs}.

CONCLUSIONS

1. The modified GC electrode with Pt nanoparticles were prepared and characterized with the available methods, for the electroreduction sensing of the investigated carboxylic acids that have significant biological and industrial importance.
2. The electroreduction of the carboxylic acids under investigation on the modified electrode with Pt nanoparticles is much more improved than that on the bare GCE.
3. CV and EIS measurements confirm that the electroreduction of the acids proceeds via EC mechanism.
4. The magnitude of the potential shift caused by the presence of the acids showed a good linear relationship with the acid dissociation constants, pK_{a1}, in the corresponding media.

ACKNOWLEDGEMENT

The authors thank Chemistry Department, Faculty of Science and Sohag University for financial support.

REFERENCES

[1] J.Jiang, A.Kucernak; J.Electroanal.Chem., **520**, 64 **(2002)**.
[2] D.A.Zhao, T.A.Peng, M.A.Liu, L.A.Lu, P.Cai; Microporous Mesoporous Mater, **114**, 166 **(2008)**.
[3] J.J.Feng, G.Zhao, J.J.Xu, H.Y.Chen; Anal.Biochem., **342**, 280 **(2005)**.
[4] J.Murbe, A.Rechtenbach, J.Topfer; Mater.Chem. Phys., **110**, 110 **(2008)**.
[5] S.Wang, Y.Yin, X.Lin; Electrochem.Commun., **6**, 259 **(2004)**.
[6] M.O.Finot, G.D.Braybrook, M.T.Mcdermott; J.Electroanal.Chem., **466**, 234 **(1999)**.
[7] J.V.Zoval, P.R.Biernacki, R.M.Penner; Anal. Chem., **68**, 1585 **(1996)**.
[8] J.V.Zoval, R.M.Stiger, P.R.Biernacki, R.M.Panner; J.Phys.Chem., **100**, 837 **(1996)**.
[9] J.V.Zoval, J.Lee, S.Gorer, R.M.Panner; J.Phys. Chem.B, **102**, 1166 **(1998)**.
[10] Z.Chen, J.Li, E.Wang; J.Electroanal.Chem., **373**, 83 **(1994)**.
[11] A.Dekanski, J.Stevanovic, R.Stevanovic, B.Z.Nikolic, V.M.Jovanovic; Carbon, **39**, 1195 **(2001)**.
[12] Z.Tang, D.Geng, G.Lu; J.Colloid Interface Sci., **287**, 159 **(2005)**.
[13] R.Kvaratskheliya, E.Kvaratskheliya; Russ.J. Electrochem., **36**, 1209 **(2000)**.
[14] Guojin Lu, Giovanni Zangari; Electrochimica Acta, **51**, 2531 **(2006)**.
[15] F.M.El-Cheikh, F.A.Rashwan, H.A.Mahmoud, Mahmoud El-Rouby; J.Appl.Electrochem., **40**, 79 **(2010)**.
[16] K.Scott; Electrochim Acta, **37**, 1381 **(1992)**.
[17] E.Stephen Treimer, H.Dennis Evans; J.Electroanal. Chem., **449**, 39 **(1998)**.
[18] Y.Xian, W.Zhang, J.Xue, X.Ying, L.Jin, J.Jin; Analyst (Lond), **125**, 1435 **(2000)**.
[19] A.L.Gopalan, K.P.Lee, K.M.Manesh, P.Santhosh, J.H.Kim; Catal.Chem., **256**, 335 **(2006)**.
[20] W.Forker; Electrochemistry, Akademie-Verlag, Berlin, **(1989)**.
[21] S.Trasatti, O.A.Petrii; Pure Appl.Chem., **63**, 711 **(1991)**.
[22] Y.Lu, M.Yang, F.Qu, G.Shen, R.Yu; Bioelectrochemistry, **71**, 211 **(2007)**.
[23] A.J.Bard, L.R.Faulkner; Electrochemical methods fundamentals and applications, Wiley, New York, **(2001)**.
[24] Ural Akbulut, Bilge Hacioglu; J.Polym.Sci., Part A: Polym.Chem., **29**, 219 **(1991)**.
[25] F.Rashwan, H.Mohran; Bull Chem.Soc.Jpn., **66**, 1871 **(1993)**.
[26] L.Pospisil, R.SoKolova, M.P.Colombini, S.Giannarelli, R.Fuoco; Microchem.J., **67**, 305 **(2000)**.
[27] S.Hrapovic, Y.Liu, K.B.Male, J.H.T.Luong; Anal. Chem., **76**, 1083 **(2007)**.
[28] R.David, E.Lide; CRC handbook of chemistry and physics, 87th Edition, Taylor and Francis, Boca Raton FL, **(2007)**.